Journal of Computational Physics **157,** 350–370 (2000)
doi:10.1006/jcph.1999.6386, available online at http://www.idealibrary.com on IDEAL®

Eigenmode Solution of 2-D and 3-D Electromagnetic Cavities Containing Absorbing Materials Using the Jacobi–Davidson Algorithm[1]

S. J. Cooke*,[2] and B. Levush†

*Institute for Plasma Research, University of Maryland, College Park, Maryland 20742; and
† Naval Research Laboratory, Code 6841, Washington, DC 20375
E-mail: {cooke, levush}@mmace.nrl.navy.mil

Received February 22, 1999; revised September 20, 1999

Eigenmodes of electromagnetic cavities containing absorbing dielectric materials are determined using an adaptation of the Jacobi–Davidson technique to solve discrete matrix eigenequations derived from Maxwell's equations. The discretisations, obtained using finite difference and finite integration methods, give rise to non-Hermitian matrices, having complex eigenvalues, and the Jacobi–Davidson method is shown to be applicable even when very low-Q cavity eigenmodes exist in the presence of highly lossy dielectric or permeable materials. Examples are given of eigensolutions for both 2-D (cylindrically symmetric) and 3-D electromagnetic operators. © 2000 Academic Press

I. INTRODUCTION

Solving Maxwell's equations in the frequency domain to obtain the electromagnetic eigenmodes of a waveguide or cavity of arbitrary shape is an important step in the design of many types of microwave and millimetre-wave components used in accelerator physics applications [1], for high-power microwave generation [2] and in passive microwave circuits. For many types of components and devices, a useful analysis may be made in the frequency domain using an eigenmode decomposition of the electromagnetic field, and often it is sufficient to consider only a small subset of these modes to obtain a comprehensive analysis of device characteristics. For example, the cavity fields may be coupled to an external

[1] The U.S. Government's right to retain a nonexclusive royalty-free license in and to the copyright covering this paper, for governmental purposes, is acknowledged.

[2] Current address: Science Applications International Corporation, McLean, VA 22102.

0021-9991/00 $35.00

system via some resonance condition that will selectively excite only modes in a particular frequency range. Eigenmode analysis of a cavity provides the resonant frequency and field distribution for each mode, and also the cavity quality (Q) if ohmic losses exist. Many numerical methods used for complex cavity eigenmode analysis fail for all but very high-Q cavities, where losses may be considered as a small perturbation to the lossless system. Mathematically, this corresponds to a departure from Hermitian matrices. In this paper we address the case where strong losses are present and demonstrate that the Jacobi–Davidson algorithm [3] can be applied successfully in this case, with a number of particular advantages for practical computations.

An example of the application of eigenmode analysis where ohmic losses must be considered is in quantifying the energy exchange that occurs in a gyroklystron device [4] during resonant interaction of cavity electromagnetic fields with a beam of charged particles, for the amplification of microwave frequency radiation. Typically the coupling to either a single mode or a small set of modes is dominant, and the interaction is strongly dependent upon the precise frequencies and Q-values of these modes. Correct calculation of ohmic losses is therefore important for an accurate simulation.

In Sections II and III, we outline the basic theory of electromagnetic eigenvalue formulations, incorporating lossy materials, and summarise methods of iterative solution. In Section IV, we describe in detail the adaptation of the recently described Jacobi–Davidson algorithm to compute a selected set of eigenvalues. In Sections V–VI, we apply the algorithm to solve a practical two-dimensional problem with ohmic loss relevant to the gyroklystron example, while in Sections VII–VIII we extend the analysis to three dimensions and apply the method to an example having very large losses.

II. THEORY

A. *Matrix Eigenvalue Formulation*

From the differential form of the continuum electromagnetic field equations a variety of useful eigenvalue formulations may be derived, depending upon the dimensionality of the system and upon constraints due to boundary conditions or imposed symmetries of the field solutions. In order to determine the eigenmodes of all but the simplest of cavity geometries, it is generally necessary to use an applicable spatial discretisation technique to approximate the field eigenequations in the problem domain using a finite representation suitable for numerical solution. Finite element, finite difference, and boundary element methods have been applied widely for this purpose, and two such methods will be used here in the examples.

To formulate a numerical eigenvalue problem, the continuum field equations are transformed using either finite difference or finite element methods to yield a linear matrix eigenequation of the generic generalised form

$$Ax_k = \lambda_k B x_k, \tag{1}$$

where A and B are discrete linear (matrix) operators, such that a finite set of components in each solution vector x_k represents a field solution corresponding to the eigenvalue λ_k. Many techniques of analysis, both direct and iterative, may be applied to solve this type of problem [5, 6]. For complex geometries the number of unknown parameters in x_k is

generally large, precluding the practical application of full-matrix methods of solution, and either direct sparse matrix or iterative solution methods are necessary.

For cases where A and B are Hermitian matrices, a number of iterative methods have been successfully applied to solve for the eigenmodes of the matrix eigenproblem. Methods include the Tückmantel algorithm [7] and subspace iteration methods based on Chebyshev polynomial acceleration [8]. These methods have been applied successfully for three-dimensional systems with large numbers of unknowns ($N \approx 10^5$–10^6) to obtain a small subset of eigenmode solutions [9].

For applications where the presence of strongly absorbing materials in a cavity is required, numerical methods used to solve for eigenmodes of lossless structures have been found to remain useful when small losses are introduced, but fail to converge when high losses are present [10]. Inverse iteration has been used to determine eigenmodes of three-dimensional cavities containing materials having loss tangents (defined below, Eq. (6)) as high as 0.4 [11]; however, long computation times were observed for the solution of a single mode. The Jacobi–Davidson method will be demonstrated here to converge well even for modes having very low Q, with materials having loss tangent as large as 1.0, and also to extract a selected set of modes from the interior of the spectrum, which can be very beneficial in practical computation.

B. *Electromagetic Theory*

An eigenvalue analysis of Maxwell's equations for electromagnetic fields in three dimensions may be derived assuming a complex representation of the real-valued physical fields with explicit oscillatory time-dependence $\exp(i\omega t)$. For example, for the electric field,

$$\begin{aligned}\vec{\mathbf{E}} &= \mathrm{Re}[\vec{E}(\vec{r})e^{i\omega t}] \\ &= \frac{1}{2}(\vec{E}(\vec{r})e^{i\omega t} + c.c.),\end{aligned} \tag{2}$$

where $c.c.$ represents the complex conjugate term. Considering only the positive frequency term, time derivatives of such fields may be simplified using the substitution $\frac{\partial}{\partial t} \rightarrow i\omega$, and Maxwell's vector field equations may be written in the symmetrical form

$$\begin{aligned}\mathrm{curl}(i\vec{H}) &= -\omega\vec{D} + i\vec{J} \\ \mathrm{curl}\,\vec{E} &= -\omega(i\vec{B}).\end{aligned} \tag{3}$$

Together with typical material constitutive relations

$$\begin{aligned}\vec{D} &= \epsilon(\vec{r})\vec{E} \\ \vec{B} &= \mu(\vec{r})\vec{H} \\ \vec{J} &= \sigma(\vec{r})\vec{E}\end{aligned} \tag{4}$$

for material permittivity $\epsilon(\vec{r})$, permeability $\mu(\vec{r})$, and conductivity $\sigma(\vec{r})$, these lead to an explicit second-order differential eigenequation in the complex vector field $\vec{E}$ and eigenvalue ω^2,

$$\mathrm{curl}\,\mu^{-1}\,\mathrm{curl}\,\vec{E} = \omega^2\left(\epsilon - i\frac{\sigma}{\omega}\right)\vec{E}. \tag{5}$$

If the material parameters ϵ and μ are real valued and the conductivity is zero in the solution domain, then this equation is of real, Hermitian form, with eigenfrequencies that are real and non-negative and eigenfields purely real. Non-physical, zero-eigenvalued, or *static*, solutions to this equation do exist, and will be discussed in Section VII.

For materials with non-zero conductivity, the absorption of electromagnetic energy due to Ohmic losses may be characterized by the loss tangent,

$$\tan\delta = \frac{\sigma}{\omega\epsilon} \tag{6}$$

which describes the fractional decrease in energy per wave period, divided by 2π. To represent energy losses in materials including those due to finite conductivity, while retaining the linear eigenvalue form, we allow complex values for material parameters ϵ and μ, rather than using σ directly. Although this leads to non-physical dispersion of material properties, it is sufficiently valid over a moderate frequency band to demonstrate our method of solution. Such loss terms break the Hermitian symmetry property and lead to complex-valued eigenfrequencies and eigenfields.

From Eq. (2), substituting for the real and imaginary parts of the complex eigenfrequency $\omega = \omega' + i\omega''$, we obtain

$$\vec{\mathbf{E}} = \mathrm{Re}[\vec{E}(\vec{r})e^{i\omega' t}]e^{-\omega'' t} \tag{7}$$

so that a positive (negative) imaginary frequency component corresponds physically to exponential decay (increase) of the modal field amplitude with time. The complex eigenfrequency may be expressed as a real-valued frequency and cavity quality factor,

$$f = \frac{\omega'}{2\pi}, \qquad Q = \frac{\omega'}{2\omega''}, \tag{8}$$

where Q is defined as 2π times the ratio of the time-averaged stored energy in the cavity to the energy loss per cycle. The factor 2 arises since the energy is proportional to the square of the field amplitude and decays as $e^{-2\omega'' t}$. For some real systems having strong losses present, the cavity-Q may become small ($\approx$1) for some modes.

The continuum eigenequation (5) may be transformed to a discrete matrix eigenequation of the form of Eq. (1), using for example the method described in Appendix A. The resulting matrix form is suitable for numerical solution as described below.

III. SOLUTION OF LARGE EIGENSYSTEMS

There are many iterative methods for the solution of large linear generalised eigenvalue problems of the form of Eq. (1) for given linear operators A and B, where in standard eigenvalue problems B is the unit matrix. These methods include inverse power iteration methods (e.g., Inverse Power Iteration, Rayleigh Quotient Iteration) and subspace iteration methods (e.g., Arnoldi, Davidson, Jacobi–Davidson, and Lanczos). The effectiveness of each method depends upon the nature of the eigenproblem, particularly the overall eigenvalue distribution, whether real or complex, and the location of the specific subset of these eigenvalues which are to be determined.

Due to the large numbers of unknowns used to discretise typical electromagnetic field eigenvalue problems, particular care must be taken with the choice and implementation of the solution algorithm so as to minimise the computational resources, both time and

storage, while obtaining convergence. Methods which may be computationally efficient when applied to small problems may scale poorly with problem size and become impractical as the number of discrete field values increases. Typically, iterative methods are most practical when the number of unknowns is large and are particularly applicable when the operator is most easily represented in functional form for numerical efficiency. With iterative methods, the number of vectors that must be stored during the solution procedure is critical and may still become a major limitation when problem size exceeds of the order of 10^6–10^7 complex unknown field values.

Subspace projection methods represent a general class of methods for the solution of large eigensystems. Such techniques generate and iteratively refine a vector subspace, represented by a set of orthonormal vectors, such that the converged subspace contains the eigenvectors corresponding to the eigenvalues of interest. The implicitly restarted Arnoldi method [12] is an algorithm of this type that has been applied to many large-scale eigenproblems. It is the basis for the subroutine library ARPACK.

Our particular method of interest for use with lossy structures is the Jacobi–Davidson technique, described recently [3, 13, 14], which has been applied to large problems in fields of quantum chemistry, acoustics, and magnetohydrodynamics [15].

IV. THE JACOBI–DAVIDSON METHOD

In outline, the Jacobi–Davidson method is an iterative subspace method, in which the large matrix problem to be solved is projected onto smaller subspaces to obtain estimated eigensolutions at each iteration. The subspaces are extended by applying an orthogonal correction procedure to selected eigensolution estimates, related to that of the Block Galerkin Inverse Iteration (BGII) method [16]. However, the correction vectors are used to *extend* the subspaces as in the Davidson method [17, 18], to promote an improved solution estimate at the next iteration. Typically, this procedure is restarted after some fixed number of iterations to limit the maximum subspace size that must be stored. The subspace is contracted to include only a few of the solution estimates that lie closest to the desired eigensolutions, and the process of subspace expansion recommences. In place of this approach, we employ a strategy in which eigenvectors associated with the least desirable eigenvalue estimates, furthest from a target eigenvalue, are removed from the subspaces at each iteration and replaced with the update vectors derived from the set of most desirable estimates. This maximises the retention of information in the subspace that can contribute to the convergence of the algorithm.

The Jacobi–Davidson technique is described here for the case of a generalised non-symmetric eigenproblem with independent left and right subspaces. The specialisation to symmetric or Hermitian matrices is straightforward once the general procedure has been outlined, but the full treatment given below underlines the separate consideration of left and right sides of the system for non-Hermitian matrices.

For systems that are not Hermitian, the left and right eigenvectors corresponding to an eigenvalue will in general not be equal, and separate subspaces should in principle be maintained and updated. This has been suggested in connection with the original Davidson method for use with non-normal matrices [18], while a generalised Lanczos solver for non-symmetric systems was introduced by Cullum *et al.* [19] using a two-sided approach to represent the left and right eigenvector solutions. In the standard Jacobi–Davidson method, for which the theory is well described by Sleijpen *et al.* [3], a single subspace is used to span the subspace of right eigenvectors and either the same subspace or one derived from

it is used for the left-subspace projection. A theory for the generalised eigenproblem using a single subspace is outlined by Booten *et al.* [15].

The stages of the Jacobi–Davidson algorithm implemented are as follows.

A. *Subspace Projection and Ritz Vectors*

The eigensystem of dimension N is projected at each iteration of the procedure into the current right and left subspaces $\mathcal{V}$ and $\mathcal{W}$, each of dimension p, where typically $p \ll N$. If the linear operators A and B are represented in some basis by $N \times N$ matrices, then the subspaces may be represented by $N \times p$ matrices $V = [v_1, \ldots, v_p]$ and $W = [w_1, \ldots, w_p]$ composed of column basis vectors spanning $\mathcal{V}$ and $\mathcal{W}$, respectively. We are seeking estimates of right-eigenvector solutions in the right-subspace $\mathcal{V}$ and of left-eigenvector solutions in the left-subspace $\mathcal{W}$, and therefore may write, for a solution k, the vectors $x_k \in \mathcal{V}$ and $y_k \in \mathcal{W}$ as the products

$$x_k = V s_k, \qquad y_k = W t_k, \tag{9}$$

where s_k and t_k are vectors of length p, and define right and left residual vectors $r_k(s_k, \theta_k)$ and $q_k(t_k, \theta_k)$ for some eigenvalue estimate θ_k,

$$r_k = A x_k - \theta_k B x_k \tag{10}$$

$$q_k^H = y_k^H A - y_k^H B \theta_k. \tag{11}$$

We next apply a Ritz procedure, requiring that the projection of the residual into the opposite subspace be zero,

$$W^H r_k = 0 \Leftrightarrow P_A s_k - \theta_k P_B s_k = 0 \tag{12}$$

$$q_k^H V = 0 \Leftrightarrow t_k^H P_A - t_k^H P_B \theta_k = 0, \tag{13}$$

where the $p \times p$ matrices

$$P_A = W^H A V, \qquad P_B = W^H B V$$

represent projections of the linear operators A and B on the pair of subspaces $\mathcal{V}, \mathcal{W}$. Equations (12) and (13) represent the corresponding right and left equations of a generalised eigenproblem for the small $p \times p$ matrices P_A and P_B. This projected eigenproblem may be solved for eigenvectors s_k and t_k and eigenvalues θ_k using a method applicable to dense matrices [20]. The vectors x_k and y_k, obtained using (9), are termed right and left Ritz vectors in the subspaces $\mathcal{V}$ and $\mathcal{W}$, respectively, corresponding to the Ritz value θ_k.

B. *Eigenvector and Ritz Vector Orthogonality*

The left and right eigenvectors of a general eigensystem possess a bi-orthogonality relation. For the simplest case where eigenvalues are distinct, pairs of non-degenerate eigensolutions satisfy

$$t_i^H P_C s_j = 0, \qquad i \neq j \tag{14}$$

for any projected matrix of the general form

$$P_C = W^H C V, \qquad C \in \{\alpha A + \beta B : \alpha, \beta \in \mathbb{C}\}. \tag{15}$$

Typically, the choice $C \equiv B$ is made, particularly when B is positive definite. For our electromagnetic eigenproblem, this corresponds to a norm based on the stored electrical energy; however, a natural choice might derive from the total electromagnetic energy instead, leading to choices $C_k = A + \omega_k^2 B$. In our examples we use the simpler form, but in the following we keep the choice of C arbitrary for generality.

In the degenerate case, sets of vectors spanning the associated invariant subspaces may be chosen such that this relation is satisfied for all vector pairs, and the same property holds.

From (9), (14), and (15), the biorthogonality relation is retained for the Ritz vectors, so that

$$y_i^H C x_j = 0, \qquad i \neq j \tag{16}$$

and therefore non-degenerate pairs of Ritz vectors are C-biorthogonal.

To improve each eigenvector estimate, we search for a correction vector orthogonal to the current Ritz vector that brings our estimate closer to the solution vector. To implement this step in the following section, we will require operators that perform this projection. Provided that C is chosen such that $y_k^H C x_k \neq 0$, we may define orthogonal projection operators

$$\mathcal{P}_k^{\perp} = I - \frac{x_k y_k^H C}{y_k^H C x_k}, \qquad \mathcal{Q}_k^{\perp} = I - \frac{C x_k y_k^H}{y_k^H C x_k}. \tag{17}$$

These operators satisfy

$$\mathcal{P}_k^{\perp 2} = \mathcal{P}_k^{\perp}, \qquad \mathcal{P}_i^{\perp} x_j = \begin{cases} 0, & i = j \\ x_j, & i \neq j \end{cases} \tag{18}$$

$$\mathcal{Q}_k^{\perp 2} = \mathcal{Q}_k^{\perp}, \qquad y_j^H \mathcal{Q}_i^{\perp} = \begin{cases} 0, & i = j \\ y_j^H, & i \neq j \end{cases} \tag{19}$$

and therefore project orthogonally to the given Ritz vector as required.

C. *Jacobi Orthogonal Component Correction*

The Jacobi–Davidson algorithm for a single subspace uses the right-hand residual vector to generate a correction vector that is orthogonal to the current Ritz vector, by obtaining an *approximate* solution to a projected linear system of equations. Typically, this is performed using a few iterations of an iterative linear solver. Since we are using separate left and right subspaces, we must generate for each Ritz value of interest a pair of correction vectors z_k and u_k that satisfy a bi-orthogonality relationship to the current right and left Ritz vectors. We solve, approximately, the two independent systems of linear equations

$$\mathcal{Q}_k^{\perp}(A - \theta_k B)\mathcal{P}_k^{\perp} z_k = -r_k, \qquad z_k \perp x_k \tag{20}$$

$$u_k^H \mathcal{Q}_k^{\perp}(A - \theta_k B)\mathcal{P}_k^{\perp} = -q_k^H, \qquad u_k \perp y_k. \tag{21}$$

The approximate solution vectors are then incorporated in the right and left subspaces, which will be used in the next iteration of the Ritz procedure.

For the efficient solution of these large projected linear systems, it is useful to observe that $r_k = \mathcal{Q}_k^{\perp} r_k$ and $q_k^H = q_k^H \mathcal{P}_k^{\perp}$, and compare (20) and (21) to preconditioned forms used in iterative solution methods [21]. Preconditioned variants of iterative solution methods which treat the left- and right-hand sides equivalently, such as the quasi-minimal residual

(QMR) [22] method or bi-conjugate gradient method (BiCG), may be adapted to solve the two related equations above in a single procedure, with the left and right preconditioning matrices replaced by the orthogonal projection operators. In our implementation, we used the QMR method, since it converges uniformly using a small set of workspace vectors. In our approximate solution we either use a fixed number of iterations or reduce the residual error by a specified factor. To achieve convergence in the lowest *overall* time, this factor is taken to be 0.1 until the solution begins to converge, then it is reduced to 0.01. Fewer iterations are used when the shift is poorly known and a very approximate solution is sufficiently valid, while quicker convergence is obtained as the eigenvalues are approached.

In principle, the rate of convergence of the Jacobi–Davidson algorithm may be greatly accelerated if a preconditioner is available to improve conditioning of this projected linear solution step [23]. In this case, the same preconditioned variant of the QMR algorithm may be applied.

The Jacobi–Davidson method expands the subspaces each step to include the newly calculated correction vectors. To limit the storage requirements, the algorithm is typically restarted after a fixed number of steps, at which point the subspace is contracted, retaining only a few Ritz vectors having Ritz values closest to the desired eigenvalue range. However, for a given amount of available storage, this procedure does not optimise the use of the information obtained at each step about the eigensolutions, and a better practice is to discard the least desirable eigensolution estimates at each step to be replaced by the new correction vectors. A similar procedure has been suggested for the Arnoldi method [12, 24]. Furthermore, for well-converged solutions the correction vector may be added directly to the corresponding subspace vector, and in practice the maximum subspace size need only exceed the desired number of solution vectors by one or two vectors. This maximises the number of solutions that may be obtained with available resources.

The complete algorithm is summarised as follows.

ALGORITHM 1. Jacobi–Davidson iteration.

Initialisation:

Select the initial subspace dimension p. Choose initial p-dimensional right and left subspaces $\mathcal{V}$ and $\mathcal{W}$ (i.e., sets of basis vectors $\{v_1, \ldots, v_p\}$, $\{w_1, \ldots, w_p\}$ spanning $\mathcal{V}$, $\mathcal{W}$, respectively) and compose matrices $V = [v_1, \ldots, v_p]$, $W = [w_1, \ldots, w_p]$ from column vectors. Specify the target convergence tolerance on the norm of the residual.

Outer Iterations:

1. Project the operators onto the subspaces; i.e., compute $p \times p$ matrices

$$P_A = W^H A V, \qquad P_B = W^H B V$$

2. Find eigensolutions (θ_k, s_k, t_k), for $k = 1 \ldots p$, to the projected left and right eigenproblems

$$P_A s_k = \theta_k P_B s_k, \qquad t_k^H P_A = t_k^H P_B \theta_k$$

and select $n \leq p$ solutions that lie closest to a target eigenvalue.

3. Calculate the Ritz vectors

$$x_k = V s_k, \qquad y_k = W t_k$$

for $k = 1 \ldots n$.

4. Calculate the right and left residuals

$$r_k = (A - \theta_k B)x_k, \qquad q_k^H = y_k^H(A - \theta_k B)$$

Identify a number $m \leq n$ of these that have not yet converged to the specified tolerance, for which correction vectors will be generated. Steps 5–6 apply to each pair of Ritz vectors to be updated (exit if $m = 0$):

5. Define orthogonal projection operators

$$\mathcal{P}_k^{\perp} = I - \frac{x_k y_k^H C}{y_k^H C x_k}, \qquad \mathcal{Q}_k^{\perp} = I - \frac{C x_k y_k^H}{y_k^H C x_k}$$

6. Inner iterative solves for correction vectors. Solve approximately the right- and left-hand linear systems

$$\mathcal{Q}_k^{\perp}(A - \theta_k B)\mathcal{P}_k^{\perp} z_k = -\mathcal{Q}_k^{\perp} r_k$$
$$u_k^H \mathcal{Q}_k^{\perp}(A - \theta_k B)\mathcal{P}_k^{\perp} = -q_k^H \mathcal{P}_k^{\perp}$$

7. Incorporate the corrections into the subspaces: Replace the subspace matrices V and W by $[x_1, \ldots, x_n, z_1, \ldots, z_m]$ and $[y_1, \ldots, y_n, u_1, \ldots, u_m]$, respectively, and C-biorthogonalise the columns, using an adapted Gram–Schmidt method. Optionally, subspace size may be reduced by including only the sums $x_k + z_k$ and $y_k + u_k$ for the updated solutions closest to convergence. Set p to the new subspace size.
8. Repeat from step 1.

D. *Complex Symmetric Eigenproblems*

For complex symmetric systems, $A = A^T$, $B = B^T$, the left eigenvectors are complex conjugates of the right eigenvectors. We may therefore use the definitions

$$W = V^* \Leftrightarrow W^H = V^T$$

so that each left-side equation becomes a transpose of the corresponding right-side equation, and only a single equation need be solved. In a numerical scheme, this may be used to reduce the storage and computation by approximately a factor of one-half, since only a single subspace need be stored and updated at each step. Hermitian systems allow a similar reduction of computation, taking $W = V$ as in the single subspace algorithm.

E. *Examples*

The examples that follow in the remainder of this paper demonstrate the effectiveness of this algorithm in identifying the solutions for electromagnetic eigenproblems. The convergence properties of an algorithm may depend upon the characteristics of the structure of the cavity and the discretisation process. For example, symmetry of the structure can lead to degeneracy of eigenvalues; materials with high loss-tangent can give rise to a spectrum having many low-Q eigenmodes; the number of unknowns in the solution may strongly influence the convergence time. The test examples are chosen to include a realistic level of complexity with regard to these criteria in order to ascertain the effectiveness of the Jacobi–Davidson algorithm for electromagnetic eigenvalue problems.

Two types of electromagnetic eigenproblems will be illustrated in this paper. First, a 2-dimensional scalar theory for symmetric TE modes of cavities having cylindrical symmetry will be used to demonstrate the eigensolution algorithm. Test examples with moderate numbers of unknowns are solved, for which eigensolutions may be determined for comparison by other means. Second, the method is applied to a full 3-dimensional vector model, based upon a finite integration method adapted from that of Bartsch *et al*. [25], for which additional computational issues that arise will be addressed.

V. THE 2-D SCALAR EIGENPROBLEM

The first class of problems that we shall use to demonstrate the algorithm relates to finding the azimuthally symmetric TE eigenmodes of cylindrically symmetric cavities having an inhomogeneous distribution of dielectric material but homogeneous permeability. In cylindrical coordinates, (r, θ, z), the azimuthal electric field is decoupled in this case, and an exact two-dimensional representation of the fields for the symmetric TE modes is obtained in terms of the single field component, $E_\theta(z, r)$, where the dielectric material is described by the dielectric function $\epsilon(z, r)$. The class includes many structures of practical application; the examples given below are taken from a four-cavity gyroklystron millimeter-wave amplifier [4], in which lossy dielectric materials are used in two of the cavities to control mode Q and field structure.

A. *Eigenvalue Formulation*

For such a circuit, an eigenvalue problem may be derived from (5) in the form of a Helmholtz equation

$$\{\nabla^2 + \omega^2 \mu \epsilon(z, r)\}[E_\theta(z, r)\hat{\theta}] = 0, \tag{22}$$

where for vectors

$$-\nabla^2 \equiv \text{curl curl} - \text{grad div}.$$

The addition of the divergence term to the operator given in (5) leaves the operator unaffected, given the assumed cylindrical symmetry, since we can apply a vector identity to ascertain the condition

$$\begin{aligned} \epsilon \text{div}\, \vec{E} &= \text{div}\, \epsilon \vec{E} - \vec{E} \cdot \text{grad}\, \epsilon \\ &= 0 \end{aligned} \tag{23}$$

in which $\text{div}\, \epsilon \vec{E} = 0$ in the absence of free charges and the vectors of the dot product are here necessarily orthogonal.

The θ-component equation may be written in the (z, r) plane as the 2-D scalar eigenproblem

$$\left\{\frac{\partial^2}{\partial z^2} + \frac{\partial^2}{\partial r^2} + \frac{1}{r}\frac{\partial}{\partial r} - \frac{1}{r^2}\right\} E_\theta = -\omega^2 \mu \epsilon(z, r) E_\theta \tag{24}$$

with boundary conditions for a closed cavity, $E_\theta = 0$ on axis and at perfectly conducting walls.

B. *Operator Symmetry*

The 2-D operator represented in Eq. (24) is not explicitly symmetric since the first-order derivative term has a spatial asymmetry. However, it is possible to obtain a symmetric form for the eigensystem by rescaling the field quantities according to an energy weighting [25]. Scaling is performed such that, at least for the loss-free case, there is a physical interpretation

$$\text{Energy} \propto E'^2$$

for the scaled field component E'.

For the operator of Eq. (24), the field may be rescaled locally as

$$E'_\theta = (r\epsilon)^{\frac{1}{2}} E_\theta$$

with the factor r arising from the azimuthal integration of the energy in cylindrical coordinates, to give a symmetric operator acting on the scaled electric field

$$\left\{\epsilon^{-\frac{1}{2}}\left[\frac{\partial^2}{\partial z^2} + \frac{\partial^2}{\partial r^2} - \frac{3}{4r^2}\right]\epsilon^{-\frac{1}{2}}\right\} E'_\theta = -\omega^2 \mu E'_\theta \tag{25}$$

in which the first order partial derivative does not appear. Scaling by the permittivity function transforms the generalised eigenproblem to a standard eigenvalue form. The cavity frequencies, ω, and mode structures, $E_\theta(z, r)$, may be obtained from the eigensolutions of this system.

C. *Discretisation*

To solve the field equations numerically we discretised the equations using the finite difference method to represent the differential operator of Eq. (25) using a 5-point stencil on an orthogonal, non-uniform, rectangular mesh. The permittivity at a solution point is taken as the volume-weighted average over the four adjacent mesh cells, each assumed to be isotropic with uniform permittivity. The symmetry of the operator is retained in the matrix representation of the discretised equations, and this was used to significant advantage in the numerical solution.

Using the representation of losses by complex values of the permittivity or permeability, the discretised equations for the symmetric eigensystems retain the same matrix form, only with some elements now complex. The matrix eigensystem using the scaled field representation for this case is *complex symmetric*.

VI. THE 2-D EXAMPLE

We will compute the symmetric modes of two cavities used in a microwave-frequency gyroklystron amplifier [4] using the Jacobi–Davidson algorithm. The amplifier operates for signal frequencies close to 94 GHz and consists of a sequence of four cavities, separated by waveguide sections, with each cavity designed to have a particular optimum frequency and Q. Resonant interaction between the cavity fields and a cyclotron electron beam in a strong axial magnetic field is the basis of the amplification process, and tolerances are such that the resonant frequency of each cavity must be controlled to within 10–30 MHz.

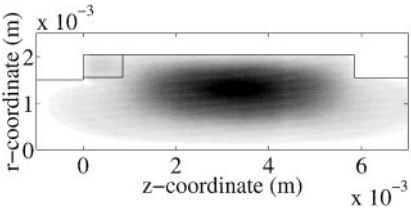

FIG. 1. Field density for the 93.52 GHz eigenmode of a cylindical gyroklystron cavity loaded by a ring of lossy ceramic material.

The frequencies of oscillation and field profiles of the cavity modes determine the efficiency, gain, and bandwidth of the gyroklystron device. To achieve the design resonant frequency and Q for each of the second and third cavities, a ring of lossy ceramic material is used to load the cylindrically symmetric cavity. Frequencies obtained here using the Jacobi–Davidson method are compared with eigenfrequencies obtained using a scattering matrix technique [26, 27] and with experimental data. Results are given in terms of frequency and Q, obtained from complex eigenvalues using (8).

Figure 1 shows the geometry and the field structure of the operating eigenmode of the second cavity, loaded with a lossy ceramic ring. The complex permittivity of the ceramic in all calculations was $\epsilon_r = 12.24 - 3.38i$, having a loss tangent, $\tan\delta = 0.276$. This value is for a composite ceramic, 80% BeO, 20% SiC at 94 GHz [28].

The Jacobi–Davidson algorithm was applied to find eigensolutions of a matrix generated using a 200×120 cell discretisation with 20,454 field values in the solution region. The technique successfully identified all of the confined symmetric eigenmodes, shown in Table I. Solutions were converged to an eigenvalue convergence error of $\approx 10^{-6}$. Even localised modes in the ceramic ring having $Q \approx 4$ were found using this technique, demonstrating the method's effectiveness for highly lossy modes. The same cavity was modelled using a scattering matrix model with a non-linear root-finding procedure, and good agreement was obtained as shown. In each method, a sufficient number of mesh points or modes was included to obtain convergence of the operating mode.

Table II demonstrates the results obtained similarly for the gyroklystron's third cavity. The Jacobi–Davidson algorithm extracted all of the eigenmodes in the frequency range of

TABLE I
Comparison for Gyroklystron Cavity No. 2 between Eigenfrequencies Calculated Here and with a Scattering Matrix Calculation

	Cavity No. 2					
	This calculation, using Jacobi–Davidson		Scattering matrix calculation		Experimental data [4]	
	Freq./GHz	Q	Freq./GHz	Q	Freq./GHz	Q
1	65.782	4.21	65.736	4.21		
2	93.519	172.20	93.520	174.73	93.59	130
3	103.43	45.47	103.41	46.19		
4	103.83	4.27	103.99	4.26		
5	115.71	38.20	115.60	39.38		

Note. Experimental data are shown for the operating mode.

TABLE II
Comparison for Gyroklystron Cavity No. 3 between Eigenfrequencies Calculated Here and with a Scattering Matrix Calculation

	Cavity No. 3					
	This calculation, using Jacobi–Davidson		Scattering matrix calculation		Experimental data [4]	
	Freq./GHz	Q	Freq./GHz	Q	Freq./GHz	Q
1	64.924	4.32	64.800	4.20		
2	92.892	174.63	92.894	175.20	93.05	128
3	102.71	45.20	102.70	46.20		
4	103.05	4.43	103.06	4.27		
5	114.83	38.03	114.74	38.80		

Note. Experimental data are shown for the operating mode.

interest. In each cavity, an experimentally determined frequency for the operating mode is shown, in reasonable agreement with the theoretical values.

VII. THE 3-D VECTOR EIGENPROBLEM

The solution of three-dimensional eigenvalue problems requires a number of additional issues to be addressed. Highly degenerate zero-frequency eigensolutions may exist that can cause numerical difficulties, and problem size is typically significantly greater. These issues must be addressed if large 3-D problems are to be solved successfully.

The eigenvalue form used for fully three-dimensional problems is a direct discretisation of Eq. (5) for a given spatial distribution of material parameters. Equation (5) permits infinitely many degenerate, zero-frequency eigensolutions, for which $\vec{E}$ takes the form of the gradient of an arbitrary scalar field. In the discretised form of the operator, one-third of the eigenvalues are zero, and this freedom can lead to numerical difficulties and even spurious solutions unless care is taken to completely decouple these static solutions from those of interest [29].

Zero-frequency solutions can also be problematic numerically for eigensolvers that specifically converge to the lowest frequency solutions such as Chebyshev polynomial iteration or simple inverse power iteration [6]. Either specific steps must be taken to suppress the unwanted modes, or else it is necessary to include a divergence term in the operator. For example, a useful choice would be

$$\operatorname{curl} \mu^{-1} \operatorname{curl} \vec{E} - \epsilon \operatorname{grad} \left\{ \frac{1}{\epsilon^2 \mu} \operatorname{div} \epsilon \vec{E} \right\} = \omega^2 \epsilon \vec{E} \tag{26}$$

which in homogeneous media reduces to the vector Helmholtz equation. For the desired modes, the additional term causes no change in the eigensolution, since from (5) these modes satisfy $\operatorname{div} \epsilon \vec{E} \equiv 0$. We have chosen the form of the additional term here so that the two sets of solutions are completely decoupled. The divergence term raises the multiply degenerate, static solutions of (5) to become eigensolutions of the independent auxiliary eigenproblem

$$-\frac{1}{\epsilon^2 \mu} \operatorname{div} \epsilon \operatorname{grad} \phi = \omega^2 \phi \tag{27}$$

for some scalar field ϕ, with $\vec{E} = -\text{grad}\,\phi$. In general, the spectrum of this auxiliary eigenproblem overlaps that of the original, polluting the desired mode spectrum and increasing the spectral density. For a given solution of the coupled problem, it is a straightforward matter to identify to which component eigenproblem it is a solution by analysis of the divergence of the eigenfield; however, this adds complexity and requires that a greater number of eigenvalues be determined initially. Alternatively, a *penalty factor* may be used to multiply the auxiliary term and scale its eigenvalues beyond the range of interest.

If eigenfrequencies interior to the spectrum may be selectively determined, such as is the case with the Jacobi–Davidson algorithm, then the issue of zero-frequency solutions is an advantage, since the static solutions are easily identified and deselected based upon an estimate of their eigenvalue. Fewer solutions need be calculated and the action of the simpler curl–curl operator is faster to compute. We therefore choose here to solve (5) rather than (26)

A. *The 3-D Finite Integration Operator*

The method applied here for the discretisation of the 3-D eigenproblem is related to the Finite Integration Method described by Bartsch *et al.* [25]. Each field is represented by averaged field quantities defined on a mesh and its associated dual mesh. The Yee cell arrangement [30] is followed, in which field components are defined on edges or faces of a regular orthogonal mesh. This arrangement is shown for a Cartesian coordinate system in Fig. 2, where the relationship between the mesh and dual mesh is apparent—each edge of the mesh intersects a face of the dual mesh, while each dual edge intersects a mesh face. A more general approach is possible using an irregular mesh, to which a similar analysis can be applied.

The discretisation of Maxwell's equations (3) using this method is detailed in Appendix A. We obtain the discretised eigensystem corresponding to (5) as the matrix equation

$$\left\{\mathcal{C}^T D_L^{-1} \mathcal{C}\right\} V = \omega^2 \{D_C\} V, \tag{28}$$

where the components of the linear vector V, having units of voltage, are elemental line-integrals of the electric field. The matrix operator $\mathcal{C}$ represents a logical curl, while

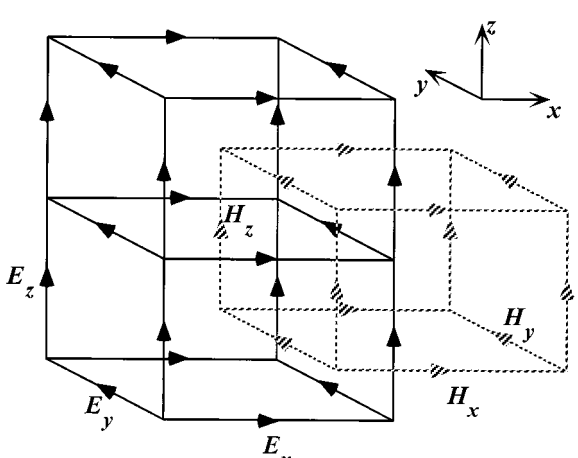

FIG. 2. Yee cell structure of 3-D discretisation. The dual grid faces intersect the midpoints of the grid edges.

diagonal matrices D_C and D_L are diagonal capacitance and inductance matrices respectively which incorporate the material and metrical details of the discretised problem.

To transform the generalised eigenproblem to a standard eigenproblem, while retaining symmetry, rescaling is performed via

$$V_j' = C_j^{1/2} V_j,$$

where C_j are the elements of the diagonal capacitance matrix, to obtain the compact symmetric form

$$\left\{ D_C^{-1/2} \mathcal{C}^T D_L^{-1} \mathcal{C} D_C^{-1/2} \right\} V' = \omega^2 V' \tag{29}$$

to be solved by numerical means. Either form of the equation may be solved using this algorithm.

VIII. THE 3-D EXAMPLES

Three-dimensional geometries increase the problem complexity in a number of ways: (a) a three-dimensional vector field increases the number of unknowns in the solution by a factor of three per cell over a scalar field, (b) many more cells are necessary to fill a three-dimensional volume while maintaining solution accuracy, (c) more coupling terms arise in the matrix operator due to greater adjacency of cells, (d) greater symmetry may exist, (e) static solutions alter the eigenvalue distribution. The following examples demonstrate the performance of the Jacobi–Davidson algorithm for the 3-D case.

A. *Cubic Cavity with High Degeneracy*

A cubic cavity with a symmetric discretisation provides an excellent test for separation of degenerate eigensolutions, so as to obtain the associated subspace. The method successfully identified the (real) eigenvalues of this structure, discretised on a $16 \times 16 \times 16$ mesh, and correctly identified even the sixfold degeneracies that exist due to the high symmetry. Eigenvalue convergence for all modes was obtained to approximately 10^{-12}, within a few orders of magnitude of the machine numerical round-off error (2×10^{-16}).

B. *Lossy Structure with Degenerate Modes*

This test example follows that of Schmitt *et al.* [10] and consists of a cavity 20 mm $\times$ 20 mm $\times$ 10 mm with a lossy dielectric block 7 mm $\times$ 7 mm $\times$ 8 mm located centrally on the square cavity floor. The dielectric constant of the block was taken as $\epsilon_r = 10 - 2i$, a loss tangent of $\tan\delta = 0.2$. Calculations were performed using a $40 \times 40 \times 30$ cell mesh, giving a discretised problem with 136,110 complex unknowns, slightly coarser than the reference example. The first ten modes were all identified successfully, with calculated eigenfrequencies in agreement with the published data as shown in Table III. Of particular note, the pairs of degenerate modes were determined provided that the initial subspace consisted of at least two independent random vectors. Since all solutions are obtained from filtering of the initial subspace, at least as many starting vectors are necessary as the degeneracy that is to be determined.

To demonstrate the convergence of the method, the solutions were permitted to converge to the limit of numerical round-off errors. Figure 3 shows the convergence history for

TABLE III
Eigenmode Solutions Obtained for the 3-D Lossy Cavity, Using a $40 \times 40 \times 30$ Cell Mesh with $\tan \delta = 0.2$

	Freq./GHz			Freq./GHz [10]	
Mode	Real	Imag.	Q	Real	Imag.
1	6.1591	0.2786	11.05	6.161	0.278
2/3	9.0888	0.7798	5.827	9.091	0.780
4/5	11.389	0.7577	7.516	11.39	0.759
6	11.412	1.0391	5.491	11.42	1.104
7	13.249	1.1596	5.713	13.25	1.161
8	13.632	0.8809	7.738	13.66	0.870
9/10	13.777	0.8640	7.973	13.78	0.860

each eigensolution. The rate of convergence is dependent upon the particular eigensolution, but is uniform for each mode, including the degenerate modes. In particular, degenerate eigenvalues exhibit very similar convergence properties, and comparison with Table III indicates convergence rates for each solution inversely proportional to the magnitude of the corresponding eigenfrequency, ω, with interior eigenvalues converging more slowly. This behaviour indicates very stable convergence properties for the Jacobi–Davidson algorithm.

In practice, it is possible to update just the solutions that have an error norm exceeding a specified threshold value, so that further convergence is suppressed, thereby minimising the computation for a particular specified level of accuracy.

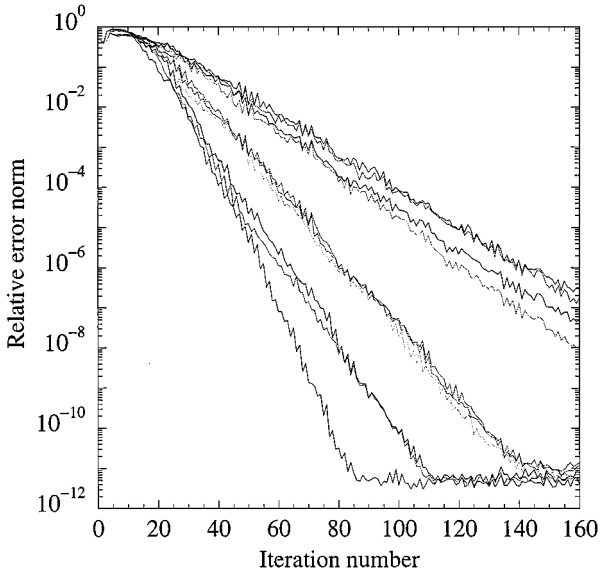

FIG. 3. Convergence history. Each trace shows the convergence of the residual norm for a single eigensolution, using a small, constant number of iterations for each linear solution step and no limit to the convergence.

TABLE IV
Eigenmode Solutions Obtained for the 3-D Lossy Cavity, Using a $40 \times 40 \times 15$ Cell Mesh with $\tan \delta = 1$

	Freq./GHz		
Mode	Real	Imag.	Q
1	5.5249	0.9077	3.043
2/3	7.4765	2.8298	1.321
4	9.2311	3.6265	1.273
5/6	9.778	3.589	1.362
7	10.82	4.185	1.292

C. *Very High Loss Structure*

To demonstrate the ability of this algorithm to handle cases of extremely high loss, the previous example was repeated with $\tan \delta = 1.0$. Table IV shows the first few eigenvalues, using a $40 \times 40 \times 15$ cell mesh for the discretisation. Although convergence time increased by a factor of four, uniform convergence was observed for each mode and eigenfrequencies were determined corresponding to $Q \approx 1$.

IX. CONCLUSION

We have applied the Jacobi–Davidson method to eigenvalue problems arising in electromagnetics in which strongly absorbing materials give rise to complex eigenvalues with a large range of both real and imaginary parts. The method has been demonstrated to successfully identify a selected set of eigenmodes of complex cavities that contain inhomogeneous distributions of absorbing dielectric material having loss tangent as large as one. By using a subspace management strategy to limit the size of the subspace without the need for a restart procedure, large eigensystems arising in the discretisation of three-dimensional problems were solved. The method has been shown to be an attractive algorithm to aid the design of microwave cavities that must incorporate strongly absorbing materials.

APPENDIX

I. Discretisation of Maxwell's Equations

To transform Maxwell's equations to a discrete orthogonal mesh, field quantities are averaged and associated with mesh components according to whether they are scalar, vector, pseudo-vector, or pseudo-scalar quantities, determined by their transformation under spatial inversion (in the language of differential forms, these correspond to 0-, 1-, 2-, and 3-forms, respectively). Scalar quantities are associated with mesh nodes, vector quantities with edges, pseudo-vectors with faces, and pseudo-scalars with the cell volume. Averaging takes place integrating over the corresponding mesh element. Field quantities associated with the dual mesh are those quantities that are derived in the transition from the microscopic to the phenomenological equations of Maxwell [31]. In this manner, the geometry inherent in Maxwell's equations for electromagnetic fields is well matched with the numerical representation, and a particularly elegant form of discretisation is obtained.

Field quantities corresponding to the mesh and dual mesh(˜) are defined as follows, having the units shown. Electric field $\vec{E}$ and magnetic field $\vec{H}$ are vector fields, represented on the mesh and dual mesh edges, respectively,

$$V_j = \int_{l_j} \vec{E} \cdot d\vec{l} \quad \text{[Voltage]}$$
$$\tilde{I}_j = \int_{\tilde{l}_j} \vec{H} \cdot d\vec{l} \quad \text{[Current]},$$

where l_j is a line element corresponding to an edge of the mesh and $\tilde{l}_j$ is a line element corresponding to an edge of the dual mesh. Magnetic induction $\vec{B}$ and electric displacement $\vec{D}$ are pseudo-vector fields, represented on the mesh and dual mesh faces, respectively,

$$\Phi_j = \iint_{A_j} \vec{B} \cdot d\vec{S} \quad \text{[Magnetic flux]}$$
$$\tilde{Q}_j = \iint_{\tilde{A}_j} \vec{D} \cdot d\vec{S} \quad \text{[Charge]},$$

where A_j is an area element corresponding to a face of a mesh cell and $\tilde{A}_j$ is an area element corresponding to a face of a dual mesh cell.

The voltage and current values obtained represent parameters analogous with electrical circuit theory. Correspondingly, the material parameters of permittivity and permeability are represented by effective capacitance and inductance values. The equivalent capacitance for each electric field component can be evaluated by considering a cell-sized capacitor along an edge, length l_j, with inhomogeneous dielectric material between faces of area $\tilde{A}_j$. The permittivity is a pseudo-scalar quantity associated with each mesh cell. For the total capacitance,

$$C_j = \frac{1}{l_j} \iint_{\tilde{A}_j} \epsilon \, dS$$
$$= \frac{1}{l_j} \sum_k \epsilon_k \tilde{A}_{jk},$$

where the sum over k combines parallel capacitances over the four mesh cells adjacent to the edge, and $\tilde{A}_{jk}$ corresponds to that part of the area element $\tilde{A}_j$ that is contained within the cell k.

The equivalent inductance for each magnetic field component may be evaluated using a similar averaging procedure, assuming a continuous B-field component and discontinuous H-field component along the edge of the dual mesh. For the effective inductance,

$$L_j^{-1} = \frac{1}{A_j} \int_{l_j} \mu^{-1} \, dl$$
$$= \frac{1}{A_j} \sum_k \frac{\tilde{l}_{jk}}{\mu_k},$$

where the sum over k corresponds to the line elements $\tilde{l}_{jk}$ in the two adjacent cells through which the dual edge element passes.

To lowest order in the discretisation length, we may represent the material constitutive relations by the corresponding circuit relations

$$\vec{D} = \epsilon \vec{E} \Rightarrow \tilde{Q}_j = C_j V_j$$
$$\vec{B} = \mu \vec{H} \Rightarrow \Phi_j = L_j \tilde{I}_j,$$

where the equivalence with electrical circuit theory is apparent. These equations relate parameters on the mesh to those of the dual mesh.

The integral forms of Maxwell's equations over the finite mesh components may be represented without approximation using the averaged quantities as follows. The curl operator for a vector field represented on the dual mesh may be evaluated using Stokes' theorem as

$$\iint_{\tilde{A}_j} (\text{curl}\, \vec{H}) \cdot d\vec{S} = \oint_{\delta \tilde{A}_j} \vec{H} \cdot d\vec{l} = \sum_k \tilde{c}_{jk} \tilde{I}_k,$$

where k ranges over the edges of the dual mesh face $\tilde{A}_j$ and the values c_{jk} define locally the direction of the integration loop with respect to the definition of the field quantities $\tilde{I}_k$,

$$\tilde{c}_{jk} = \begin{cases} +1 & \text{same direction} \\ -1 & \text{opposite direction.} \end{cases}$$

Similarly, for the curl operator acting on a vector field represented on the mesh,

$$\iint_{A_j} (\text{curl}\, \vec{E}) \cdot d\vec{S} = \oint_{\delta A_j} \vec{E} \cdot d\vec{l} = \sum_k \hat{c}_{jk} V_k$$

with $\hat{c}_{jk}$ defined similarly to $\tilde{c}_{jk}$ above. Divergence and gradient operators may be similarly defined on both the mesh and the dual mesh; however, we do not require them here.

It is possible to define global matrices to represent the two curl operators, denoted $\tilde{\mathcal{C}}$ and $\mathcal{C}$, respectively, and it can be shown that $\tilde{\mathcal{C}} = \mathcal{C}^T$ [25].

We may now represent, in matrix form, Maxwell's equations (3) for oscillatory fields in the absence of currents as

$$\mathcal{C}^T (i\tilde{I}) = -\omega D_C V$$
$$\mathcal{C}\, V = -\omega D_L (i\tilde{I}),$$

where D_C and D_L are diagonal matrices of the capacitance and inductance terms, respectively.

We therefore obtain the discretised eigensystem as the matrix equation

$$\left\{\mathcal{C}^T D_L^{-1} \mathcal{C}\right\} V = \omega^2 \{D_C\} V$$

which is of the generalised matrix eigenform.

ACKNOWLEDGMENTS

This work was supported by the U.S. Office of Naval Research. We thank Dr. A. Mondelli, SAIC, for his help during the preparation of this paper.

REFERENCES

1. T. Weiland, Time domain electromagnetic field computation with finite difference methods, *Int. J. Numer. Model. Electron. Networks Devices Fields* **9**, 295 (1996).
2. T. M. Antonsen, Jr., A. A. Mondelli, B. Levush, J. P Verboncoeur, and C. K. Birdsall, Advances in modeling and simulation of vacuum electronic devices, *Proc. IEEE* **87**(5), 804 (1999).
3. G. L. G. Sleijpen and H. A. van der Vorst, A Jacobi–Davidson iteration method for linear eigenvalue problems, *SIAM J. Matrix Anal. Appl.* **17**(2), 401 (1996).
4. M. Blank, B. G. Danly, B. Levush, P. E. Latham, and D. E. Pershing, Experimental demonstration of a W-band gyroklystron amplifier, *Phys. Rev. Lett.* **79**(22), 4485 (1997).
5. G. H. Golub and C. F. Van Loan, *Matrix Computations*, Johns Hopkins Series in the Mathematical Sciences (Johns Hopkins Univ. Press, Baltimore, 1989), Vol. 3.
6. O. Axelsson, *Iterative Solution Methods* (Cambridge Univ. Press, Cambridge, UK, 1996).
7. J. Tückmantel, An improved version of the eigensolver SAP applied in URMEL, *CERN/RF* **85**(4), (1985).
8. Y. Saad, Tchebyshev acceleration techniques for solving non-symmetric eigenvalue problems, *Math. Comp.* **42**, 567 (1984).
9. D. Schmitt and T. Weiland, 2D and 3D computations of eigenvalue problems, *IEEE Trans. Magn.* **28**(2), 1793 (1992).
10. D. Schmitt, R. Schuhmann, and T. Weiland, The complex subspace iteration for the computation of eigenmodes in lossy cavities, *Int. J. Numer. Model. Electron. Networks Devices Fields* **8**, 385 (1995).
11. D. Schmitt, B. Steffen, and T. Weiland, 2D and 3D computations of lossy eigenvalue problems, *IEEE Trans. Magn.* **30**(5), 3578 (1994).
12. D. C. Sorensen, Implicit application of polynomial filters in a k-step Arnoldi method, *SIAM J. Matrix Anal. Appl.* **13**(1), 357 (1992).
13. A. Booten and H. A. van der Vorst, Cracking large-scale eigenvalue problems. Part I. Algorithms, *Comput. Phys.* **10**(3), 239 (1996).
14. A. Booten and H. A. van der Vorst, Cracking large-scale eigenvalue problems. Part II. Implementations, *Comput. Phys.* **10**(4), 331 (1996).
15. A. Booten, D. Fokkema, G. Sleijpen, and H. A. van der Vorst, Jacobi–Davidson methods for generalised MHD-eigenvalue problems, *Z. Angew. Math. Mech.* **76**(S1), 131 (1996).
16. J. Descloux, J.-L. Fattebert, and F. Gygi, Rayleigh quotient iteration, an old recipe for solving modern large-scale eigenvalue problems, *Comput. Phys.* **12**(1), 22 (1998).
17. E. R. Davidson, The iterative calculation of a few of the lowest eigenvalues and corresponding eigenvectors of large real symmetric matrices, *J. Comput. Phys.* **17**, 87 (1975).
18. E. R. Davidson, Super-matrix methods, *Comput. Phys. Comm.* **53**, 49 (1989).
19. J. Cullum, W. Kerner, and R. Willoughby, A generalised nonsymmetric Lanczos procedure, *Comput. Phys. Comm.* **53**(1–3), 19 (1989).
20. W. H. Press, S. A. Teukolsky, W. T. Vetterling, and B. P. Flannery, *Numerical Recipes in FORTRAN*, 2nd ed. (Cambridge Univ. Press, Cambridge, UK, 1992).
21. R. Barrett, M. Berry, T. F. Chan, J. Demmel, J. Donato, J. Dongarra, V. Eijkhout, R. Pozo, C. Romine, and H. Van der Vorst, *Templates for the Solution of Linear Systems: Building Blocks for Iterative Methods* (SIAM, Philadelphia, 1994).
22. R. W. Freund and N. M. Nachtigal, An implementation of the QMR method based on coupled 2-term recurrences, *SIAM J. Sci. Comput.* **15**(2), 313 (1994).
23. G. L. G. Sleijpen, H. A. van der Vorst, and E. Meijerink, Efficient expansion of subspaces in the Jacobi–Davidson method for standard and generalised eigenproblems, *Electron. Trans. Numer. Anal.* **7**, 75 (1998).
24. M. N. Kooper, H. A. van der Vorst, S. Poedts, and J. P. Goedbloed, Application of the implicitly updated Arnoldi method with a complex shift-and-invert strategy in MHD, *J. Comput. Phys.* **118**, 320 (1995).
25. M. Bartsch *et al.*, Solution of Maxwell's equations, *Comput. Phys. Comm.* **72**, 22 (1992).

26. J. M. Neilson, P. E. Latham, M. Caplan, and W. G. Lawson, Determination of the resonant frequencies in a complex cavity using the scattering matrix formulation, *IEEE Trans. Microwave Theory Tech.* **37**(8), 1165 (1989).
27. P. E. Latham, Dielectric lined waveguides, unpublished.
28. M. Afsar, Tufts University, private communication.
29. B. Jiang, J. Wu, and L. A. Povinelli, The origin of spurious solutions in computational electromagnetics, *J. Comput. Phys.* **125**, 104 (1996).
30. K. S. Yee, Numerical solution of initial boundary value problems involving Maxwell's equations in isotropic media, *IEEE Trans. Antenn. Propag.* **14**, 302 (1966).
31. G. Scharf, *From Electrostatics to Optics*, Texts and Monographs in Physics (Springer-Verlag, Berlin, 1994).